A QUASI-RANDOM PHASE CONTROL AS A NEW OPEN-LOOP ACTIVE CONTROL METHOD

Haecheon Choi*
School of Mechanical and Aerospace Engineering, Seoul National University,
Seoul 151-742, KOREA
choi@socrates.snu.ac.kr

Seongwon Kang, Jeongyoung Park and Jinsung Kim
School of Mechanical and Aerospace Engineering, Seoul National University,
Seoul 151-742, KOREA

ABSTRACT

The objective of the present study is to increase mixing in turbulent flows behind a backward-facing step and downstream of a jet exit using a newly-developed quasi-random phase (QRP) control method. In this method, spatially sinusoidal but temporally varying blowing and suction with zero-net mass flux are provided at the edge of the backward-facing step and the jet exit. Large eddy simulations are conducted for both flows. It is shown that the velocity and vorticity fluctuations substantially increase downstream of the QRP control, indicating significant increases in mixing behind the backward-facing step and downstream of the jet exit. The results of the QRP control are compared with those of single frequency actuation and spatially sinusoidal blowing/suction (stationary in time or moving at a constant phase speed in the spanwise/azimuthal direction), showing the largest mixing in the case of QRP control.

INTRODUCTION

Mixing enhancement has been one of the most important problems in fluid mechanics. Therefore, many attempts have been made to increase mixing by passive and active means for various flow fields such as jet, mixing layer, and flow behind a backward-facing step. Among those passive and active control methods, the periodic blowing and suction (i.e. at a specific frequency) from a slot or a speaker is an attractive control method because there is no net mass flux provided into the flow field. In general, it has been found that the growth of roll-up vortices and their interaction like pairing are enhanced at a certain range of actuation frequencies and mixing is increased. Readers may refer to Sigurdson (1995) for a review on the periodic forcing in various geometries.

Researches about plane mixing layer have shown that the most commonly-observed flow structures in this flow are the primary roll-up vortices and the secondary streamwise vortices. These streamwise rib vortices together with pairing of roll-up vortices play an important role of increasing entrainment (Lasheras *et al.* 1986; Bell & Mehta 1990, 1993). The interesting connection between the streamwise rib vortices and entrainment has attracted researchers to utilize this concept for mixing control. Nygaard & Glezer (1994) and Collis *et al.* (1994) imposed time-harmonic excitation having spanwise-non-uniform phase or frequency distributions on developing mixing layer. They observed mixing enhancement and the 'chain-link-fence' vortical structure which is different from the usual rib/roller vortex found in plane mixing layer. Bell & Mehta (1990) generated spanwise perturbations upstream of mixing layer, to investigate how the imposed organized streamwise vortices change the entrainment process in turbulent mixing layer. They observed the entrainment increase in the near-field region but the decrease in the far-field region, because the streamwise vortices imposed disturbed the standard pairing process.

Researches conducted for mixing layer suggest that generating streamwise vortices in the flow field may be a possible control strategy of increasing mixing. In the previous studies for mixing enhancement the following

*Also at Center for Turbulence and Flow Control Research, Institute of Advanced Machinery and Design, Seoul National University. This work is supported by the Creative Research Initiatives of the Korean Ministry of Science and Technology.

three different open-loop control methods were considered: (1) spatially uniform but temporally periodic blowing and suction (Case A); (2) spatially sinusoidal but temporally stationary blowing and suction (Case B); (3) spatially sinusoidal blowing and suction but moving at a constant phase speed in the spanwise/azimuthal direction (Case C).

In the present study, we want to achieve larger mixing by introducing a newly-developed QRP control in which the blowing and suction is spatially sinusoidal but temporally varying with keeping zero-net mass flux. The QRP control method is applied to two different flows: (1) turbulent flow over a backward-facing step; (2) circular jet. The results of the QRP control are compared with those from the previous three control methods. The turbulent flow fields are generated using the large eddy simulation (LES) technique with a dynamic subgrid-scale model (Germano *et al.* 1991; Lilly 1992).

QUASI-RANDOM PHASE CONTROL

In this study, we suggest a new open-loop control method for mixing enhancement, based on a quasi-random phase function as follows: for flow over a backward-facing step,

$$\phi(z,t) = A_0 \sin[\frac{2\pi}{L_z}(z + z_p(t))], \quad (1)$$

$$z_p(t) = U\alpha < \sum_i \mathrm{Rand}_i(t) >, \quad (2)$$

and for circular jet,

$$\phi(\theta,t) = A_0 \sin(\theta + \theta_p(t)), \quad (3)$$

$$\theta_p(t) = U\alpha < \sum_i \mathrm{Rand}_i(t) >, \quad (4)$$

where ϕ is the control input (blowing and suction), z (or θ) is the direction along the actuation slot, A_0 is the amplitude ($0.1U$ for flow over the backward-facing step and $0.05U$ for circular jet), L_z is the wave length of the control input, $\mathrm{Rand}_i(t)$ (random value) is generated at each time interval $\triangle t_r$, and α is a scaling parameter. $\langle\rangle$ denotes a low-pass filter which is used to eliminate small-scale wiggles of $z_p(t)$ (or $\theta_p(t)$) in time: the elimination of wiggles is performed only for the physical implementation, i.e. smooth variation of the phase in time is easier to realize in practical applications. We found that two phases with and without filtering produced essentially the same result.

An important point of the QRP control method in (1) - (4) is that the control input varies sinusoidally in space and quasi-randomly in time, but keeping zero-net mass flux. This QRP control is applied to two different flow fields for mixing enhancement using large eddy simulation: flow over a backward-facing step and circular jet.

Three other open-loop control methods described before, whose results are compared with those of the QRP control method, can be expressed as follows:

$$\phi(t) = A_0 \sin(2\pi f t) \text{ for Case A}, \quad (5)$$

$$\phi(z) = A_0 \sin(\frac{2\pi}{L_z} z) \text{ for Case B}, \quad (6)$$

$$\phi(z,t) = A_0 \sin[\frac{2\pi}{L_z}(z + V_p t)] \text{ for Case C1}, \quad (7)$$

$$\phi(\theta,t) = A_0 \sin(\theta + \frac{V_p}{d} t) \text{ for Case C2}, \quad (8)$$

where f is the actuation frequency and V_p is the phase speed. For all the control cases considered, the mass fluxes of blowing and suction averaged in time and space are zero, and the rms values are kept the same.

For Case A, the actuation (blowing/suction) changes only in time, providing a periodic spanwise/azimuthal vorticity to the flow. On the other hand, for Case C and QRP control, the actuation changes both in time and space (spanwise/azimuthal direction). Therefore, the streamwise vorticity ($\partial v/\partial z \neq 0$ or $\partial v/\partial\theta \neq 0$) as well as the spanwise/azimuthal vorticity is generated at the slot from the actuation, letting us expect more mixing with these control methods than the other two cases. Here, v is the wall-normal velocity.

NUMERICAL METHODS

Turbulent flow over a backward-facing step

The numerical scheme to solve the unsteady three-dimensional Navier-Stokes equations is essentially the same as that used by Akselvoll & Moin (1995). The Crank-Nicolson method is used for the convection and diffusion terms in the wall-normal direction, and a third-order Runge-Kutta method is used for all the other terms. The nonlinear equation resulting from the implicit treatment of the convection term is linearized without losing the second-order time accuracy. The second-order central difference is used for all the terms in a staggered grid system.

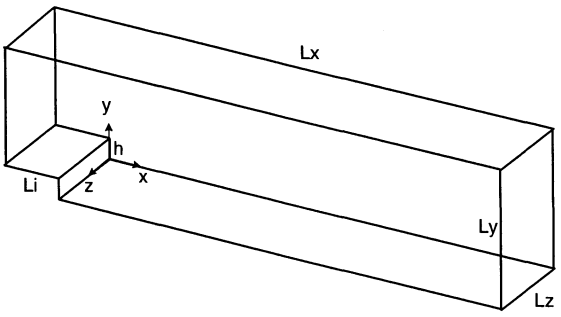

Figure 1: Schematic of the computational domain for flow over a backward-facing step.

Figure 1 shows the schematic diagram of the computational domain, where (x=0, y=h) is the location of the backward-facing step edge. The computational domain size in each direction is L_i=2.5h, L_x=22.5h, L_y=6h and L_z=4h, respectively, which is nearly similar to that used in Le *et al.* (1997). The Reynolds number based on the free-stream velocity U and step height h is 5100 and the Reynolds number based on the free-stream velocity and displacement thickness δ^* at x=-2.5h is 1058.

The number of grid points used is 151×56×64 in the streamwise, wall-normal and spanwise directions, respectively. In the wall-normal direction, thirty-two grids are used at $y \leq h$, and thirty-eight grids are used in the streamwise direction at the inlet section before the step ($x \leq 0$). The total number of grid points used here is about twice that used in Akselvoll & Moin (1995).

The no-slip condition is used at the wall, and the periodic boundary condition is used in the spanwise direction. At $y = L_y$, the following no-stress condition is used assuming symmetry at the upper boundary (Le *et al.* 1997): $\partial u/\partial y = 0$, $v = 0$, $\partial w/\partial y = 0$. The blowing/suction slot is located at $-0.1h \leq x \leq 0$ and y=h. The angle of actuation is 45° with respect to the streamwise direction. The boundary condition at the exit is the convective outflow condition, $\partial u_i/\partial t + U_c \partial u_i/\partial x = 0$, where U_c is the plane-averaged streamwise velocity at the exit. For the present computation, a separate LES of turbulent boundary layer flow is performed to provide realistic inlet turbulence at x=-2.5h based on the method by Lund *et al.* (1998). The computational time step used is $\Delta t = 0.015h/U$.

Jet

The numerical method used to solve the unsteady three-dimensional Navier-stokes equations in cylindrical coordinate is based on a semi-implicit fractional step method (Akselvoll & Moin 1995). The computational domain is decomposed into two regions: core region and outer region. Within each region only the derivatives in one direction is treated implicitly, i.e., derivatives in the azimuthal direction within core region and derivatives in the radial direction within outer region, respectively. All terms are resolved with the second-order central difference scheme in space.

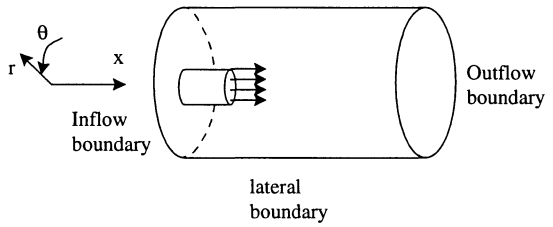

Figure 2: Schematic of the computational domain for jet.

Figure 2 shows a schematic diagram of the computational domain. The Neumann condition, $\partial u_i/\partial x = 0$, is used at the outflow boundary and at the inflow boundary except the jet exit extruding into the computational domain, where a top-hat velocity profile is specified. At the lateral boundary $\partial r u_r/\partial r = 0$ and $\omega_\theta = \omega_z = 0$ are used. Ambient fluid is entrained from the inflow boundary as well as from the lateral boundary. The Reynolds number based on the nozzle diameter d and the uniform velocity at the pipe exit U is 10,000.

The number of grid points used is 288 × 80 × 96 in the streamwise (x), radial (r), and azimuthal (θ) directions, respectively. The computational domain size is ($26d, 7d$) in (x, r) directions. The computational time step used is $\Delta t = 0.02d/U$.

RESULTS

Turbulent flow over a backward-facing step

The single frequency actuation (Case A) is conducted at $fh/U = 0.2$ (equation (5)), which is known to be an effective non-dimensional frequency in increasing mixing in this flow (Chun & Sung 1996). For Case B (equation (6)), $L_z = 4h$ is considered (see below). The phase speed for Case C1 (equation (7)) is taken to be $V_p = 0.8U$, at which the actuation at any spanwise location has the blowing/suction frequency of $fh/U = 0.2$. The QRP control, (1) and (2), has three parameters: the first is the spanwise wavelength for the actuation, L_z, the second is the time interval between random-value generations, Δt_r, and the third is the scaling parameter α.

First, a parametric study is performed

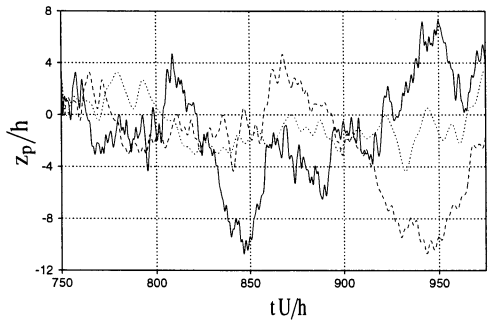

Figure 3: Examples of quasi-random phases (α=0.3): ———, $\triangle t_r$=0.03h/U; – – – –, $\triangle t_r$=0.06h/U; ·····, $\triangle t_r$=0.12h/U. Note that the spanwise domain length is $4h$ and thus the periodicity in z should be applied to z_p >$4h$ and z_p <0.

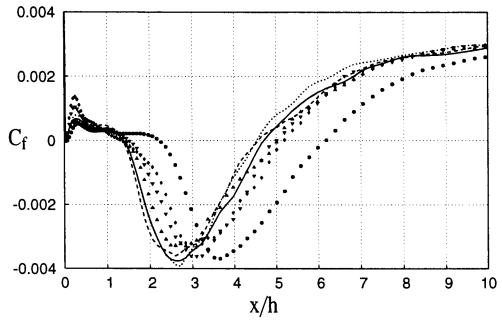

Figure 4: Friction coefficients: •, uncontrolled; ▲, QRP control with $\triangle t_r$=0.03h/U and α=0.12; ▼, $\triangle t_r$=0.06h/U and α=0.12; ♦, $\triangle t_r$=0.12h/U and α=0.12; ———, $\triangle t_r$=0.03h/U and α=0.3; – – – –, $\triangle t_r$=0.06h/U and α=0.3; ·····, $\triangle t_r$=0.12h/U and α=0.3.

for the parameters $\triangle t_r$ and α with L_z=4h: $\triangle t_r$=0.03, 0.06 and 0.12h/U, and α=0.12 and 0.3. Figure 3 shows the quasi-random phases generated at $\triangle t_r$=0.03, 0.06 and 0.12h/U with α=0.3. As shown in figure 3, increasing $\triangle t_r$ increases the time scale of the phase (i.e. slow movement of the phase in the spanwise direction), but the amplitudes of the phase are the same for different $\triangle t_r$'s due to constant α. On the other hand, increasing α with constant $\triangle t_r$ not only increases the amplitude of the phase but also increases the movement speed of the phase in the spanwise direction.

For flow over a backward-facing step, the reattachment length (C_f = 0) has been considered as one of the indices in representing mixing behind the backward-facing step. Figure 4 shows the friction coefficients of six QRP controls, together with that of the uncontrolled flow. For the uncontrolled case, the reattachment length (X_r) is 6.2h. It is seen that the reduction of the reattachment length depends more on α than on $\triangle t_r$ for the parameter ranges investigated in this study. For the most successful QRP control, X_r becomes about 4.5h. The best QRP control result is

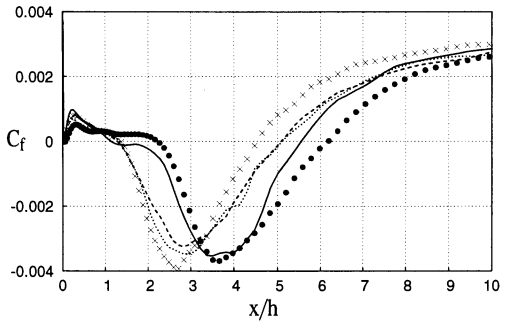

Figure 5: Variation of the friction coefficient due to different control methods: •, uncontrolled; – – – –, Case A (fh/U = 0.2); ———, Case B; ·····, Case C1 (V_p = 0.8U); ×, QRP control ($\triangle t_r$=0.12h/U and α=0.3).

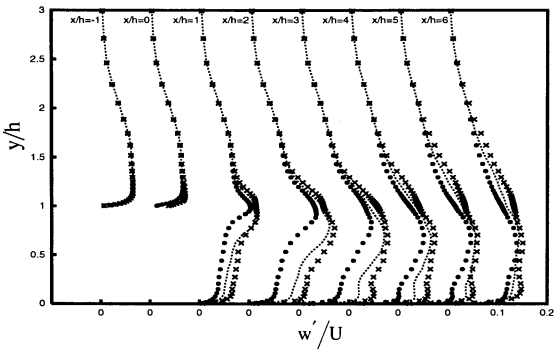

Figure 6: RMS spanwise velocity fluctuations: •, uncontrolled; – – – –, Case A (fh/U = 0.2); ×, QRP control ($\triangle t_r$=0.12h/U and α=0.3).

compared with those of Cases A, B and C1 in figure 5. It is clear that the successful QRP control ($\triangle t_r$ = 0.12h/U and α=0.3) reduces the reattachment length most among the control methods considered.

So far, we have used L_z=4h. Because the performance of the QRP control in reducing X_r depends also on L_z, we tried two more L_z's, 2h and 8h with $\triangle t_r$=0.12h/U and α=0.3. In the case of L_z=2h, X_r was about 5.4h, while it was about 4.9h in the case of L_z=8h. Therefore, the case with L_z=4h reduced the reattachment length most among three different spanwise wavelengths.

Figure 6 shows the rms spanwise velocity fluctuations with and without controls. The rms spanwise velocity fluctuations significantly increase due to the successful QRP control. The same behavior was also observed in the other velocity fluctuations and the vorticity fluctuations.

Figure 7 shows the time sequence of the pressure iso-surfaces for the QRP control, together with the blowing/suction profile at each instance. Each iso-surface of the low pressure is considered as a vortical structure (Robinson 1991). It is clear that inclined vortical struc-

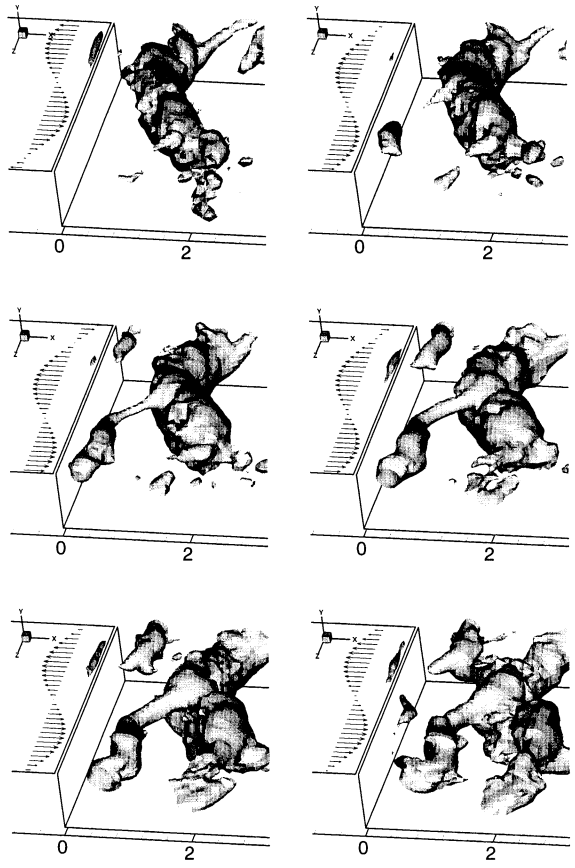

Figure 7: Time sequence of the pressure iso-surfaces for the QRP control. The vectors before the step denote the blowing/suction profile at each instance. Here, the arrow heading downstream denotes the blowing, and that heading upstream the suction. Time increases from left to right and from top to bottom.

tures are generated near the step as the blowing/suction profile traverses in the spanwise direction. These inclined vortical structures have two components. One is the spanwise roll-up vortex which is generated by local blowing and suction, and the other is the streamwise-vorticity component generated by tilting of the spanwise vorticity due to the phase movement in the spanwise direction. The irregular phase movement of the blowing/suction profile shown in figure 3 generates various sizes of inclined vortical structures. These vortical structures get closer due to different convection velocities and interact among themselves in the downstream (figure 7). This vortical interaction increases mixing and reduces the reattachment length.

Jet

The actuation (the radial velocity) is provided at the jet exit. The QRP control method ($\alpha = 0.2\pi$ and $\Delta t_r = 0.02d/U$) is applied to circular jet for mixing enhancement. The single frequency actuation (Case A; equation (6))

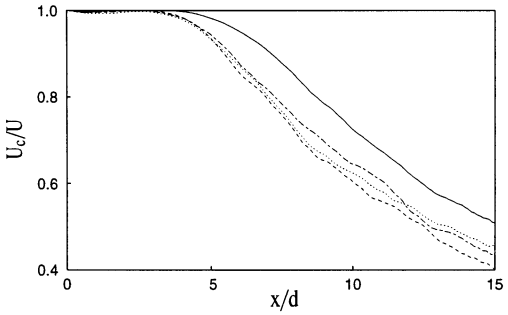

Figure 8: Variation of the mean streamwise velocity along the jet axis: ———, no control; ·····, Case A; — — —, Case C2; – – – –, QRP control.

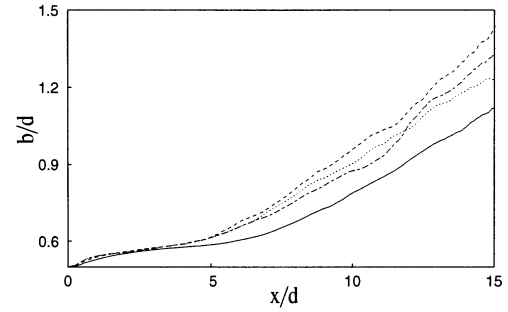

Figure 9: Variation of the jet half width in the streamwise direction: ———, no control; ·····, Case A; — — —, Case C2; – – – –, QRP control.

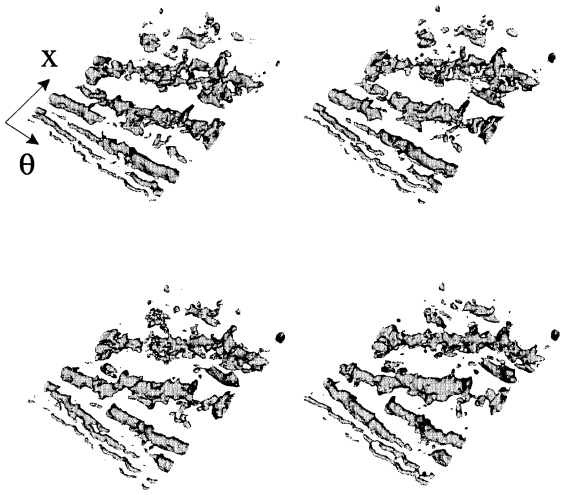

Figure 10: Time sequence of the pressure iso-surfaces for the QRP control. Here the iso-surfaces are unfolded in the azimuthal direction. Time increases from left to right and from top to bottom.

is conducted at $fd/U = 0.85$, which is known to be an effective non-dimensional frequency in increasing mixing in jet flow (Zaman & Hussain 1980). Case B is not considered in this flow because we want to obtain uniform mixing in the azimuthal direction and Case B does not provide uniform mixing in θ. The phase speed for Case C2 (equation (8)) is taken to be $V_p = 2\pi \times 0.85U$, at which the actuation at any

azimuthal location has the blowing/suction frequency of $fd/U = 0.85$.

Figure 8 shows the variation of the mean streamwise velocity along the jet axis. It is clear that the QRP control reduces the mean velocity most rapidly along the jet axis among the control methods investigated. The velocity and vorticity fluctuations also increase most rapidly along the jet axis for the QRP control (not shown here). Figure 9 shows the jet half width in the streamwise direction, indicating largest mixing for the QRP control.

Figure 10 shows the time sequence of the pressure iso-surfaces for the QRP control. Again, it is clear that inclined vortical structures are generated near the jet exit as the blowing/suction profile traverses in the azimuthal direction. Therefore, the mechanism of mixing enhancement by the QRP control in this flow is very similar to that in flow over the backward-facing step.

CONCLUSION

In the present study, we suggested a new active open-loop control method for mixing enhancement. In this method, the blowing and suction profile from a slot was a sine function in the spanwise/azimuthal direction whose phase changed quasi-randomly (so was called 'quasi-random-phase' (QRP) control).

The QRP control was applied to turbulent flow over a backward-facing step and circular jet. It was shown that the velocity and vorticity fluctuations substantially increased downstream of the control, indicating significant increases in mixing. The results of the QRP control were also compared with those of single frequency actuation and spatially sinusoidal blowing/suction (stationary in time or moving at a constant phase speed in the spanwise/azimuthal direction), showing the largest mixing in the case of the QRP control.

References

Akselvoll, K., and Moin, P., 1995, "Large eddy simulation of turbulent confined coannular jets and turbulent flow over a backward facing step", *Report* No. TF-63, Department of Mechanical Engineering, Stanford University.

Bell, J. H., and Mehta, R. D., 1990, "Development of a two-stream mixing layer from tripped and untripped boundary layers", *AIAA J.*, Vol. 28, pp. 2034–2042.

Bell, J. H., and Mehta, R. D., 1993, "Effects of imposed spanwise perturbations on plane mixing-layer structure", *J. Fluid Mech.*, Vol. 257, pp. 33–63.

Chun, K. B., and Sung, H. J., 1996, "Control of turbulent separation flow over a backward-facing step by local forcing", *Exps. Fluids*, Vol. 21, pp. 417–426.

Collis, S. S., Lele, S. K., Moser, R. D., and Rogers, M. M., 1994, "The evolution of a plane mixing layer with spanwise nonuniform forcing", *Phys. Fluids*, Vol. 6, pp. 381–396.

Germano, M., Piomelli, U., Moin, P., and Cabot, W. H., 1991, "A dynamic subgrid-scale eddy viscosity model", *Phys. Fluids* A, Vol. 3, pp. 1760–1765.

Lasheras, J. C., Cho, J. S., and Maxworthy, T., 1986, "On the origin and evolution of streamwise vortical structures in a plane, free shear layer", *J. Fluid Mech.*, Vol. 172, pp. 231–258.

Le, H., Moin, P., and Kim, J., 1997, "Direct numerical simulation of turbulent flow over a backward-facing step", *J. Fluid Mech.*, Vol. 330, pp. 349–374.

Lilly, D. K., 1992, "A proposed modification of the Germano subgrid-scale closure method", *Phys. Fluids* A, Vol. 4, pp. 633–635.

Lund, T. S., Wu, X., and Squires, K. D., 1998, "Generation of turbulent inflow data for spatially-developing boundary layer simulations", *J. Comp. Phys.*, Vol. 140, pp. 233–258.

Nygaard, K. J., and Glezer, A., 1994, "The effect of phase variations and cross-shear on vortical structures in a plane mixing layer", *J. Fluid Mech.*, Vol. 276, pp. 21–59.

Robinson, S. K., 1991, "The kinematics of turbulent boundary layer structure", *NASA Tech. Mem.* 103859.

Sigurdson, L. W., 1995, "The structure and control of a turbulent reattaching flow", *J. Fluid Mech.*, Vol. 298, pp. 139–165.

Zaman, K. B. M. Q., and Hussain, A. K. M. F., 1980, "Vortex pairing in a circular jet under controlled excitation. Part 1. General jet response", *J. Fluid Mech.*, Vol. 101, pp. 449–491.